

# Self-Healing Thermosensitive Hydrogel for Sustained Release of Dexamethasone for Ocular Therapy

Ada Annala, Blessing C. Ilochonwu, Danny Wilbie, Amir Sadeghi, Wim E. Hennink, and Tina Vermonden\*



Cite This: *ACS Polym. Au* 2023, 3, 118–131



Read Online

ACCESS |



Metrics & More



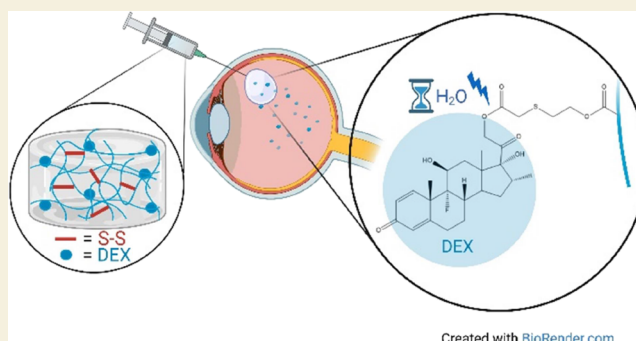
Article Recommendations



Supporting Information

**ABSTRACT:** The aim of this study was to develop an injectable hydrogel delivery system for sustained ocular delivery of dexamethasone. To this end, a self-healing hydrogel consisting of a thermosensitive ABA triblock copolymer was designed. The drug was covalently linked to the polymer by copolymerization of methacrylated dexamethasone with *N*-isopropylacrylamide (NIPAM) and *N*-acryloxysuccinimide (NAS) through reversible addition–fragmentation chain transfer (RAFT) polymerization, using poly(ethylene glycol) (PEG) functionalized at both ends with a chain transfer agent (CTA). Hydrogel formation was achieved by mixing aqueous solutions of the formed thermosensitive polymer (with a cloud point of 23 °C) with cystamine at 37 °C, to result in covalent cross-linking due to the reaction of the *N*-hydroxysuccinimide (NHS) functionality of the polymer and the primary amines of cystamine. Rheological analysis showed both thermogelation and covalent cross-linking at 37 °C, as well as the self-healing properties of the formed network, which was attributed to the presence of disulfide bonds in the cystamine cross-links, making the system injectable. The release of dexamethasone from the hydrogel occurred through ester hydrolysis following first-order kinetics in an aqueous medium at pH 7.4 over 430 days at 37 °C. Based on simulations, administration of 100 mg of hydrogel would be sufficient for maintaining therapeutic levels of dexamethasone in the vitreous for at least 500 days. Importantly, dexamethasone was released from the hydrogel in its native form as determined by LC–MS analysis. Cytocompatibility studies showed that at clinically relevant concentrations, both the polymer and the cross-linker were well tolerated by adult retinal pigment epithelium (ARPE-19) cells. Moreover, the hydrogel did not show any toxicity to ARPE-19 cells. The injectability of the hydrogel, together with the long-lasting release of dexamethasone and good cytocompatibility with a retinal cell line, makes this delivery system an attractive candidate for treatment of ocular inflammatory diseases.

**KEYWORDS:** dexamethasone for ocular drug delivery, pNIPAM-based hydrogels, injectable hydrogels, RAFT polymerization, intravitreal pharmacokinetics



Created with BioRender.com

## 1. INTRODUCTION

Intravitreal injection is currently the best choice for drug administration into the posterior segment of the eye, as both topical and systemic drug delivery routes are severely hindered due to the physiological barriers of the eye.<sup>1–3</sup> However, even after intravitreal injection, ocular drug delivery of therapeutics is challenged by the short retention times of the drugs in the vitreous, which leads to the need for repeated injections, especially in the case of chronic diseases that require long-term treatments.

Dexamethasone is a common clinically used anti-inflammatory therapeutic for the treatment of various ocular diseases, such as diabetic retinopathy, (diabetic) macular edema, retinal vein occlusion and other age-related and inflammatory intraocular diseases.<sup>3,4</sup> Due to its relatively short half-life of 3–6 h in the vitreous after intravitreal injections, the urgent need for sustained release systems achieving a prolonged

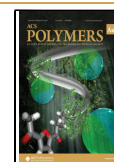
therapeutic effect is evident.<sup>3,5</sup> Additionally, repeated intravitreal injections, while generally considered safe, cause a significant burden to the society, and moreover, to the individual patients themselves, compromising patient compliance.<sup>1,6</sup> Currently, there is only one poly(lactic-co-glycolic acid) (PLGA) implant-based sustained release formulation for intraocular delivery of dexamethasone on the market<sup>7</sup> while other formulations, such as hydrogel and polymeric nanomaterial-based delivery systems are being developed.<sup>3,8–12</sup> However, there is still a need for delivery systems for

**Received:** August 19, 2022

**Revised:** October 21, 2022

**Accepted:** October 21, 2022

**Published:** November 3, 2022



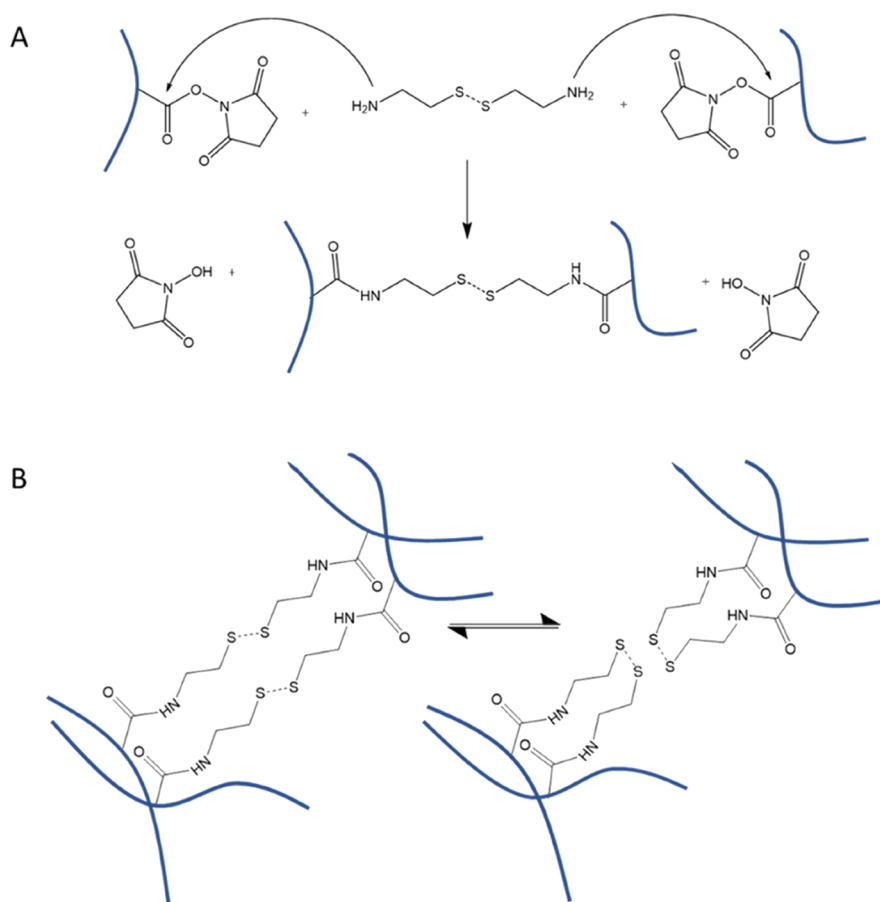


**Figure 1.** (A) Cross-linking mechanism between the NAS functionality of the polymer (blue) and CA. (B) Self-healing mechanism of the hydrogel after applying mechanical stress is based on dynamic disulfide exchange reaction.

dexamethasone to the posterior segment, which are biodegradable, can be administered intravitreally through G30–32 needles, and release dexamethasone over several months.

In recent years, the self-healing properties of hydrogels cross-linked by dynamic covalent bonds, including disulfide bonds, have been studied, especially for the development of injectable hydrogels suitable for drug delivery and tissue engineering purposes.<sup>13,14</sup> Under mechanical stress, these hydrogels show reduced viscosity that recovers once the stress is removed. With hydrogels cross-linked by disulfide bonds, the self-healing properties have been shown to be the result of disulfide exchange (Figure 1).<sup>13–17</sup>

The reaction between disulfide-containing cystamine (CA) and *N*-acryloxysuccinimide (NAS) (Figure 1) was previously exploited to form reversibly cross-linked thermosensitive polymeric micelles.<sup>18</sup> In the present study, the disulfide cross-linking mechanism was applied for cross-linking triblock copolymers aimed for the development of an injectable thermosensitive hydrogel for sustained delivery of dexamethasone. To incorporate dexamethasone into the hydrogel, a dexamethasone prodrug with methacrylate functionality and hydrolysable sulfide ester was synthesized and characterized according to a previously reported method.<sup>19</sup> We used reversible addition–fragmentation chain transfer (RAFT) polymerization to copolymerize this dexamethasone prodrug with *N*-isopropylacrylamide (NIPAM) and NAS using a poly(ethylene glycol) (PEG) RAFT macro chain transfer agent (CTA). The synthesized triblock copolymer as well as the obtained hydrogel after the cross-linking with CA was

characterized, and the release of dexamethasone in an aqueous medium was studied. Finally, the cytocompatibility of the hydrogel was evaluated.

## 2. MATERIALS AND METHODS

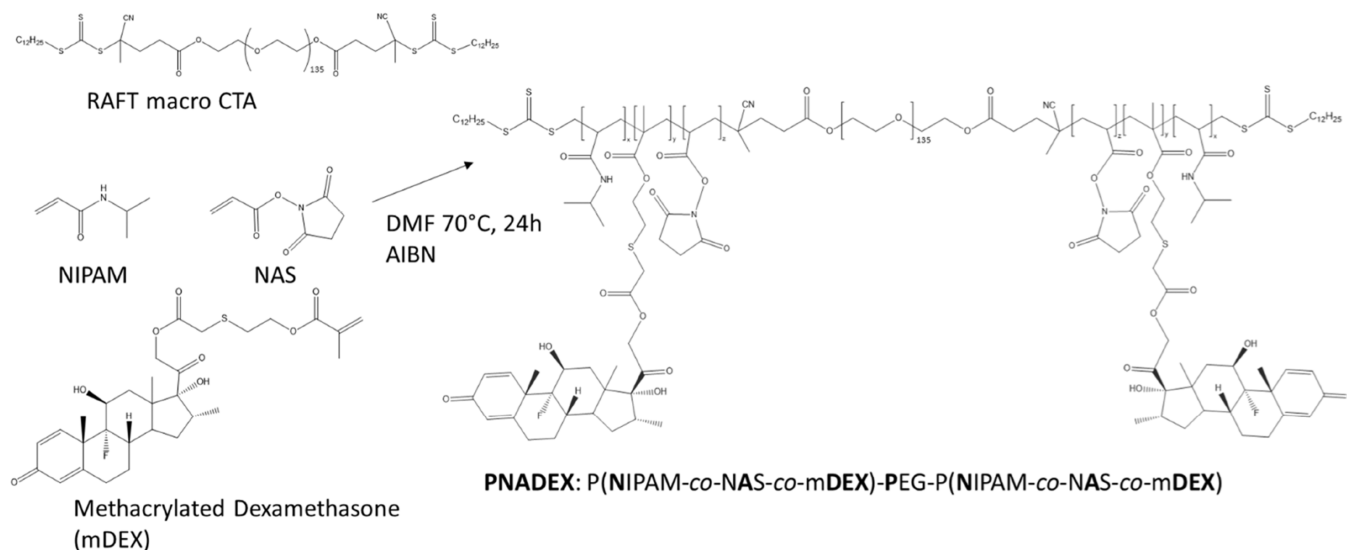
All chemicals were obtained from Sigma-Aldrich (Zwijndrecht, the Netherlands) and used as received, unless indicated otherwise. Dichloromethane ( $\text{CH}_2\text{Cl}_2$ ) was obtained from Biosolve (Valkenswaard, the Netherlands) and 4-dimethylaminopyridine (DMAP) was purchased from Fluka (Zwijndrecht, the Netherlands). Concentrated phosphate buffered saline (PBS) (pH 7.4) was purchased from Fisher Scientific (Fisher BioReagents, Thermo Fisher Scientific, Waltham, MA, USA) and diluted 10 times with MilliQ water prior use (final composition: 11.9 mM phosphates, 137 mM sodium chloride, 2.7 mM potassium chloride).

### 2.1. Synthesis of Bifunctional PEG<sub>6000Da</sub> Macro CTA for RAFT Polymerization

The synthesis of double sided PEG<sub>6000Da</sub> macro CTA was achieved through Steglich esterification<sup>20</sup> using *N,N'*-dicyclohexylcarbodiimide (DCC) as a coupling agent and 4-dimethylaminopyridine (DMAP) as a catalyst according to a method previously reported with some modifications<sup>21</sup> (Supporting Information, Scheme S1).

Briefly, PEG<sub>6000Da</sub> (1.00 g, 0.167 mmol), 4-cyano-4-[(dodecylsulfanylthiocarbonyl) sulfanyl]pentanoic acid (RAFT CTA) (168 mg, 0.42 mmol), and DMAP (6.1 mg, 0.050 mmol) were dissolved in dry DCM (10 mL) on ice and purged with nitrogen gas while protected from light. Next, DCC (103 mg, 0.50 mmol) was dissolved in dry DCM (10 mL) on ice and this solution was subsequently added dropwise in about 5 min under a nitrogen atmosphere while stirring. The reaction mixture was removed from the ice bath and allowed to

## Scheme 1. Synthesis Route of PNADEX



slowly reach room temperature. After 16 h stirring, the milky dispersion was filtered through a 0.2  $\mu\text{m}$  Phenex PTFE syringe filter (Phenomenex, Aschaffenburg, Germany) to remove the formed 1,3-dicyclohexylurea precipitate, and the polymer was collected by precipitation in ice cold diethylether (DEE) followed by filtration (filter paper, catalogue number 516-0297, VWR International BV, Amsterdam, the Netherlands) to collect the crude product. To remove traces of unreacted RAFT CTA, the product was dialyzed against dimethylsulfoxide (DMSO) for 1 day at room temperature and subsequently against water for 4 days at 4  $^{\circ}\text{C}$  (MWCO 3.5 kDa, Spectra/Por 45 mm, Carl Roth, Karlsruhe, Germany) and lyophilized. The synthesized macroinitiator as well as PEG<sub>6000Da</sub> were characterized by gel permeation chromatography (GPC) and  $^1\text{H}$  NMR analysis. The degree of functionalization of the obtained PEG<sub>6000Da</sub> RAFT macro CTA was determined with  $^1\text{H}$  NMR by addition of trichloroacetyl isocyanate (TAIC) to determine the amount of unreacted OH groups.<sup>22</sup>

## 2.2. Synthesis of p(NIPAM-co-NAS)-PEG-P(NIPAM-co-NAS) (PNA)

PEG<sub>6000Da</sub> RAFT macro CTA (25 mg, 3.7  $\mu\text{mol}$ ), *N*-isopropylacrylamide (NIPAM) (117 mg, 1.03 mmol), and acrylic acid *N*-hydroxysuccinimide ester (NAS) (8.0 mg, 47  $\mu\text{mol}$ ) were dissolved in 1 mL of dry *N,N*-dimethylformamide (DMF). Next, 48  $\mu\text{L}$  of azobisisobutyronitrile (AIBN) stock (5.0 mg/mL in dry DMF) was added, and the mixture was purged with nitrogen gas at RT. The polymerization was carried out at 70  $^{\circ}\text{C}$  for 24 h under a nitrogen atmosphere and constant stirring. The formed polymer was precipitated in ice cold DEE and collected after centrifugation for 10 min at 4  $^{\circ}\text{C}$  and 10,000 g. The supernatant was removed, and the remaining solvent was evaporated under reduced pressure. The precipitation process was repeated three times and the obtained polymer was dried overnight at RT and collected as a white solid with a slight yellow tint. Finally, the polymer was characterized using GPC and  $^1\text{H}$  NMR analysis.

## 2.3. Synthesis of the Methacrylated Dexamethasone Prodrug (mDEX)

Dexamethasone with methacrylated thioether functionality was synthesized according to a protocol described previously<sup>19</sup> (Supporting Information, Scheme S2) and characterized by  $^1\text{H}$  NMR and ultra-performance liquid chromatography (UPLC).

## 2.4. Synthesis of p(NIPAM-co-NAS-co-mDEX)-PEG-P(NIPAM-co-NAS-co-mDEX) (Abbreviated as PNADEX)

The synthesis route of PNADEX is shown in Scheme 1. PEG<sub>6000Da</sub> RAFT macro CTA (30 mg, 4.4  $\mu\text{mol}$ ), NIPAM (144 mg, 1.27 mmol), NAS (14.0 mg, 82.8  $\mu\text{mol}$ ), and mDEX (18.2 mg, 31.5  $\mu\text{mol}$ ) were dissolved in 1.5 mL of dry *N,N*-dimethylformamide (DMF). Next, 58  $\mu\text{L}$  of AIBN stock solution (5.0 mg/mL in dry DMF) was added and the mixture was purged with nitrogen gas at RT. The polymerization was carried out at 70  $^{\circ}\text{C}$  for 24 h under a nitrogen atmosphere and constant stirring. The polymer was precipitated in ice cold DEE and collected after centrifugation for 10 min at 4  $^{\circ}\text{C}$  and 10,000 g. The supernatant was removed, and remaining solvent was evaporated under reduced pressure. To remove solvent traces of DMF, the crude product was dialyzed against DMSO for 2 days (MWCO 3.5 kDa, Spectra/Por 45 mm, Carl Roth, Karlsruhe, Germany) followed by freeze-drying. The dry polymer was reconstituted in water (1 h in 4  $^{\circ}\text{C}$ ) and freeze-dried to obtain a white fluffy powder with a yield of 78%. Finally, the polymer was characterized using GPC and  $^1\text{H}$  NMR analysis.

## 2.5. NMR Spectroscopy

NMR spectra were recorded using an Agilent 400-MR NMR spectrometer (Agilent Technologies, Santa Clara, CA, USA). Approximately 5 mg of analyte was dissolved in 0.6 mL of deuterated solvent. Either DMSO- $\text{D}_6$  ( $\delta = 2.50$  ppm) or  $\text{CDCl}_3$  ( $\delta = 7.26$  ppm) was used as solvent, and the chemical shifts of analytes were calibrated according to the residual solvent peaks visible in the spectra.

## 2.6. Gel Permeation Chromatography

GPC was performed to determine the number average molecular weight ( $M_n$ ) and molecular weight distribution of the synthesized polymers and the RAFT macro CTA. A Waters Alliance System (Waters Corporation, Milford, MA, USA) equipped with a refractive index detector and a mixed-D column (Polymer Laboratories, Agilent Technologies, Santa Clara, CA, USA) at 65  $^{\circ}\text{C}$  was used. An eluent of 10 mM LiCl in DMF was used as a mobile phase with a flow rate of 1 mL/min. Samples were dissolved in the eluent with a concentration of 5.0 mg/mL and filtered before analysis over a 0.2  $\mu\text{m}$  PTFE filter (Whatman Mini-UniPrep G2 syringeless filter, Sigma-Aldrich). A series of linear PEGs with narrow and defined molecular weights (PSS GmbH, Mainz, Germany) were used as calibration standards.

## 2.7. Determination of the Cloud Point

The cloud point (CP) of the polymers was measured with a Jasco FP-8300 spectrofluorometer (Tokyo, Japan). The polymer was dissolved overnight in PBS in a concentration of 3 mg/mL at 4  $^{\circ}\text{C}$ . The



temperature was increased from 4 to 50 °C and afterward returned to 4 °C with a rate of 0.5 °C/min. The scattering intensity of the polymeric solution was measured at 650 nm and the CP is defined as the onset of increasing scattering intensity.<sup>23</sup>

### 2.8. Formation of the Hydrogel

To form 100 mg of 10 wt % hydrogel, 10 mg of PNADEX or PNA was first dissolved in 80  $\mu$ L of PBS at 4 °C. For cross-linking, 10  $\mu$ L of cystamine (CA) stock solution (38 and 45 mg/mL for PNA and PNADEX, respectively) in borate buffered saline (BBS, 9.0 g/L NaCl, 6.0 g/L Na<sub>2</sub>B<sub>4</sub>O<sub>7</sub>, 7.4 g/L H<sub>3</sub>BO<sub>3</sub>, pH 9.0) was added to the polymer solution, vortexed, and incubated at 37 °C for at least 3 h. The CA stock solutions were prepared with a concentration matching the NHS functionality of the polymers. Briefly, the molar ratio of amine groups in CA to NHS groups in the polymer was adjusted to be 1:1. Gel formation was confirmed by a vial tilting test after 3 h incubation in 37 °C followed by 1 h incubation in 4 °C. As a control, the vial tilting test was carried out on polymer solutions without a cross-linker, where 10  $\mu$ L of BBS was used in place of CA stock solution.

### 2.9. Swelling and Degradation

PNA (44 mg) was dissolved in 352  $\mu$ L of PBS, followed by addition of 44  $\mu$ L of CA stock solution prepared as described in Section 2.8 to yield a 10 wt % polymer solution. The formed solution was mixed and transferred into a mold with cylindrical inserts (2.8 mm radius and 1 mm height) resulting in hydrogels of approximately 25  $\mu$ L ( $n = 6$ ). The hydrogels were allowed to form for 3 h at 37 °C and subsequently transferred into 1.5 mL glass vials. The weight of the gels was recorded and 500  $\mu$ L of PBS was added as the swelling medium followed by incubation at 37 °C. At different time points, the PBS medium was removed, and the weights of the gels were recorded. Afterward, 500  $\mu$ L of fresh PBS was added and the gels were further incubated at 37 °C. The weights of the gels were compared to their initial weights to obtain swelling and degradation degrees over time. After 20 days, 500  $\mu$ L of 10 mmol tris(2-carboxyethyl)phosphine (TCEP) in PBS (pH 7.4) was added to three of the gels to trigger cleavage of the disulfide bonds in the cross-linker. After 45 min incubation at 37 °C, the weights of the gels were recorded again. The final weights were recorded 2 h after addition of TCEP.

### 2.10. Rheological Characterization

The rheological properties of the hydrogels (150  $\mu$ L) were analyzed using a Discovery HR-2 Hybrid Rheometer (TA Instruments, Etten-Leur, the Netherlands) with a 20 mm aluminum plate geometry (gap 200  $\mu$ m) and a Peltier plate, equipped with a solvent trap. Polymer solution was introduced in the rheometer directly after addition of the CA solution and mixing at 4 °C. The storage and loss moduli,  $G'$  and  $G''$  respectively, were recorded with a strain of 0.1% and a frequency of 1.0 rad/s over a temperature gradient from 4 to 37 °C, with a 1 °C/min heating rate. The hydrogel was kept at 37 °C for 30 min, followed by frequency sweep from 0.1 to 100 rad/s and subsequently  $G'$  and  $G''$  were recorded over a temperature gradient from 37 to 4 °C. The linear viscoelastic regime was established with a strain increasing from 0.01 to 1000% at 37 °C. Strain and recovery experiments were carried out after gel formation at 37 °C with a strain of 0.1% and a frequency of 1.0 rad/s. The strain was increased to 800% for 2 min, followed by applying a strain of 0.1% for 20 min.  $G'$  and  $G''$  were recorded over repeated high–low strain cycles. As a control, in addition to hydrogels cross-linked by CA, the rheological characterization was carried using a cross-linker that does not contain disulfide bonds. Briefly, hydrogels were prepared as described in Section 2.8; however, 80  $\mu$ L of PNADEX polymeric solution was mixed with 10  $\mu$ L of hexamethylenediamine dissolved in BBS (37 mg/mL).

### 2.11. Release of Dexamethasone from the Hydrogel and Intravitreal Pharmacokinetics Simulation

Hydrogels of 100 mg ( $n = 3$ ) were prepared using PNADEX as described in Section 2.8 in 1 mL cylindrical glass vials, with diameter of 8 mm (clear glass test tubes, ROTILABO, Carl Roth, Karlsruhe, Germany). After gel formation, 500  $\mu$ L of prewarmed 37 °C PBS supplemented with 1% Tween 80 (to solubilize released dexametha-

sone) and 0.02% NaN<sub>3</sub> (to prevent bacterial growth) was added as the release medium and the gels were incubated at 37 °C. At predetermined time points, 200  $\mu$ L of samples were withdrawn followed by the addition of the same volume of the fresh release medium. The medium was refreshed on average every 4–5 days. After 80 days, the volume of the release medium was increased to 700  $\mu$ L to prevent mechanical damage to the soft gels during medium refreshments. The collected release samples were stored at –20 °C until analysis with UPLC. Noteworthy, the isolated bovine vitreous was also used as the release medium in a parallel experiment. However, it was impossible to retain constant pH values in these samples and therefore no reliable data could be obtained.

To quantify the released dexamethasone, 10  $\mu$ L of DMSO was added to 100  $\mu$ L of the release samples to ensure complete dissolution of the released dexamethasone and the obtained solution was centrifuged at 25,000  $\times$  g for 15 min at room temperature to remove any particulate impurities. The supernatant was collected (70  $\mu$ L) and analyzed using an Acquity UPLC (Waters Corporation, Milford, MA, USA) equipped with a UPLC CSH C18 column (100  $\times$  2.1 mm, 1.7  $\mu$ m, 130 Å, Waters Corporation). Gradient elution was achieved using 5% acetonitrile (MeCN) in water as eluent A and 100% MeCN as eluent B. Both eluents contained 1% perchloric acid (PCA) as a pH modifier. The injection volume was 5  $\mu$ L, the flow rate was 0.75 mL/min, and the gradient run from 0 to 100% B in 7 min. Dexamethasone was detected at 246 nm and the concentrations of the drug in the different release samples were quantified using a calibration curve of 0.5–100  $\mu$ g/mL dexamethasone in MeCN. Results were analyzed using Empower Software (Version 3-FRS, Waters Corporation) and GraphPad Prism (GraphPad Software, USA, Version 9.1). Curve fitting was done in Python 3.10.2 using SciPy 1.8.0 least\_squares optimization functionality.<sup>24</sup>

The obtained in vitro release rate constant ( $k$ ) of dexamethasone from the PNADEX-CA hydrogel was used for simulation of intravitreal pharmacokinetics of dexamethasone in humans. Pharmacokinetics were simulated using a compartmental model reported and validated in the literature for vitreal kinetics of sustained release of dexamethasone from nanomaterials (Supporting Information, Figure S1)<sup>25,26</sup> using the parameters shown in Table S1. When applicable, parameters for dexamethasone phosphate were used in the model, due to the lack of available reported kinetic parameters for dexamethasone in the literature. The model assumes first-order dexamethasone release kinetics from the hydrogel, and it is assumed that all covalently linked dexamethasone in the hydrogel is releasable. The volume of injection (90  $\mu$ L, corresponding to approximately 100 mg of hydrogel) and the dose of dexamethasone (623  $\mu$ g) were used in the simulation, and in addition, the vitreal kinetics for bolus injection of dexamethasone solution with the same dose were simulated as a control. STELLA software (v. 8.1.1) (ISEE systems, USA) and the fourth-order Runge–Kutta algorithm were used for the simulations.

### 2.12. Hydrolysis of Methacrylated Dexamethasone and Stability of Dexamethasone in the Aqueous Medium

Stock solutions of dexamethasone or mDEX (1 mg/mL in DMSO) were diluted to 0.1 mg/mL with 1.8 mL of PBS pH 7.4, BBS pH 8.0, or BBS pH 9.0 and incubated at 37 °C for 2 weeks. The buffers contained 1% Tween 80 as the solubilizer and 0.02% NaN<sub>3</sub>. At predetermined time points, 200  $\mu$ L of samples were collected and stored at –20 °C until analysis with UPLC as described in Section 2.11.

### 2.13. Mass Spectrometry of Dexamethasone Degradation Products

Stock solutions of dexamethasone or mDEX (1 mg/mL, 200  $\mu$ L) were diluted to 0.1 mg/mL with 1.8 mL of PBS pH 7.4, BBS pH 8.0, or BBS pH 9.0 and incubated at 37 °C for 48 h. The samples were diluted 1:1 with MeCN and filtered through a 0.2  $\mu$ m syringe filter and 100  $\mu$ L was collected for analysis. Liquid chromatography mass spectrometry (LC–MS) analysis was performed using Bruker micrOTOF electrospray ionization MS (Bruker Daltonics, Billerica, MA, USA) equipped with a SunFire C18 column (4.6  $\times$  150 mm, 5



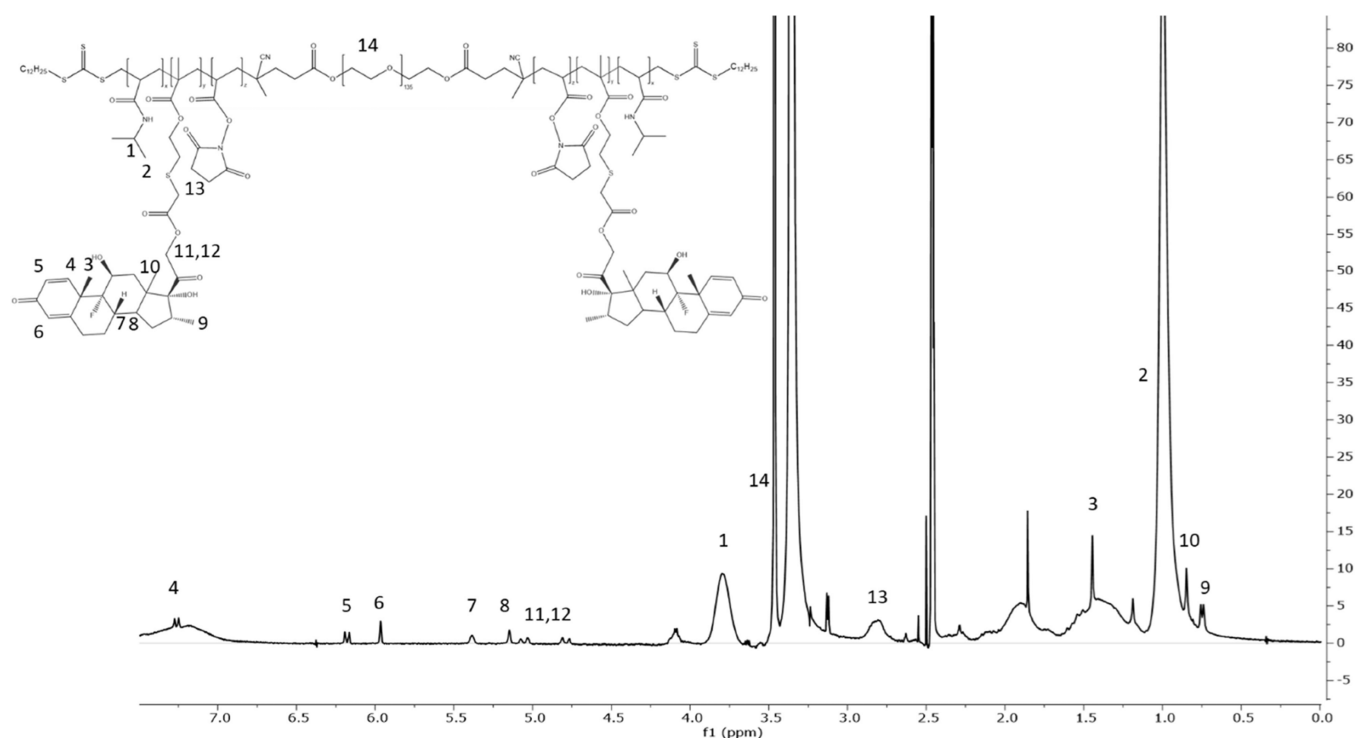


**Figure 2.**  $^1\text{H}$  NMR spectrum of PNADEX in  $\text{DMSO}-d_6$ . Residual solvent peaks are observed at 2.50 ppm (DMSO) and 3.33 ppm ( $\text{H}_2\text{O}$ ).

$\mu\text{m}$ , 100 Å, Waters Corporation, Milford, MA, USA). A gradient of MeCN from 5 to 100% in water in 30 min was used with 0.1% formic acid in the mobile phase as the modifier. The flow rate was 0.5 mL/min, with a total runtime of 50 min. The data handling and analysis were executed using Bruker DataAnalysis software version 4.0 (Bruker Daltonics).

#### 2.14. Cytocompatibility of PNADEX and CA

Retinal pigment epithelium derived ARPE-19 cells (catalog number CRL 2302) were obtained from ATCC and maintained in Dulbecco's modified Eagle medium/nutrient mixture F-12 (DMEM/F-12) (Gibco, Thermo Fisher Scientific, Waltham, MA, USA) supplemented with 10% FBS and 1% L-glutamine. The cells were maintained under fully humid conditions at 37 °C and 5%  $\text{CO}_2$  and used for experiments between passage numbers 13 and 20.

For the alamarBlue assay, cells were seeded into Greiner CELLSTAR 96-well black polystyrene plates #655090 (Greiner Bio-One GmbH, GE), and for the live-dead staining in Greiner CELLSTAR 96-well black glass bottom plates #665090 (Greiner Bio-One GmbH, GE) at a density of 32,000 cells/ $\text{cm}^2$ . The cells were allowed to attach for 24 h, followed by incubations with series dilutions of polymers dissolved in the respective complete cell culture media at concentrations between 0.125 and 5 mg/mL ( $n = 3$ ). The cytotoxicity of the cross-linker CA was evaluated at concentrations between 0.0625 and 0.5 mg/mL for the alamarBlue assay and 0.015 and 1 mg/mL for the live-dead assay, dissolved in the complete growth medium ( $n = 3$ ).

**2.14.1. alamarBlue Cytotoxicity Assay.** Cells were exposed to treatment conditions for 24 h, after which the medium was replaced with complete medium containing 10% alamarBlue reagent (500  $\mu\text{M}$  Resazurin sodium salt in PBS). Negative controls ( $n = 3$ ) for dead cells (incubated with 1% Triton X-100 for 15 min prior incubation with the medium containing the alamarBlue reagent) and positive controls ( $n = 3$ ) of living cells incubated in the complete medium were included in the assay. The background was corrected against wells with the complete medium containing 10% alamarBlue reagent, incubated without cells ( $n = 3$ ) and the fluorescence intensities were normalized against the positive control. The plates were further incubated at 37 °C for 3 h and covered from direct light. The fluorescence was measured with a fluorescence excitation wavelength

of 550 nm and an emission wavelength of 590 nm using a FLUOstar OPTIMA plate reader (BMG Labtech GmbH, Ortenberg, Germany). The cell viability of the treated cells was evaluated through their metabolic activity.

**2.14.2. Live-Dead Staining Cytocompatibility.** For the live-dead assay, living cells were stained green by conversion of the nonfluorescent calcein acetoxy methyl ester (Calcein AM) to green fluorescent calcein inside the cells, while permeable dead cells were stained red in the nuclei with propidium iodide (PI). The cells were exposed to treatment conditions for 24 h, after which the medium was replaced with a complete medium containing 3  $\mu\text{M}$  Calcein AM (Cayman Chemical Company, MI, USA) and 25  $\mu\text{M}$  PI (Invitrogen, Thermo Fisher Scientific). The plates were incubated for an additional 30 min. Negative controls for dead cells (incubated with 1% Triton X-100 for 15 min prior staining) and positive controls of living cells without treatments stained with single dyes were included in the assay.

The cells were imaged using a Yokogawa CellVoyager CV7000 confocal microscope (Yokogawa, Tokyo, Japan). Images were acquired at 20 $\times$  magnification and 2  $\times$  2 binning was applied. Calcein was excited using the 490 nm laser of the microscope and imaged in the BP525/40 channel of the microscope using 11 ms exposure time. PI was excited for 100 ms using the 590 nm laser and imaged in the BP600/37 channel.

Image analysis was performed using Columbus (PerkinElmer, version 2.7.1) and representative overlays were prepared using ImageJ (version 1.52p), using the settings specified in Supporting Information, Table S2. Dead cells were identified by the nucleus staining in the 600 nm channel, and live cells were identified by the 525 nm cytosolar signal. Both were counted using the in-built Columbus analysis method specified in Supporting Information, Table S3. The percentage of live cells was calculated by pooling all fields in a well as a single datapoint and averaging the result between two wells ( $n = 2$ ). Cell viability differences between polymer dosages in the alamarBlue and live/dead cell staining data were analyzed in GraphPad version 9.3.1 by one-way ANOVA and multiple comparisons with Tukey post hoc correction.

**Table 1. Characteristics of PNA and PNADEX Synthesized by RAFT**

polymer	feed ratio NIPAM:NAS:mDEX	copolymer composition <sup>a</sup> NIPAM:NAS:mDEX	$M_n^a$ (kDa)	$M_n^b$ (kDa)	$\bar{D}^b$	CP (°C)	yield (%)	amount of dexamethasone (wt %) <sup>c</sup>
PNA	93:7:0	92:8:0	36.9	16.7	1.47	32	81	N/A
PNADEX	82:8:10	81:8:11	37.1	16.0	1.53	23	78	6.3 <sup>c</sup>

<sup>a</sup>Determined by <sup>1</sup>H-NMR. <sup>b</sup>Determined by GPC. <sup>c</sup>The amount of native dexamethasone was calculated based on the molar ratio of mDEX incorporated in the PNADEX triblock copolymer.

### 2.15. Gel Cytocompatibility

For evaluating the cytocompatibility of the cross-linked hydrogel, 50  $\mu$ L of 10% PNADEX-CA hydrogel was formed as described in Section 2.8 in a well of a 24-well plate (Greiner CELLSTAR glass bottom 24-well plate, #662892) ( $n = 2$ ). During gel formation, the plate was tilted, allowing the gel to cover approximately 1/3 of the well surface area. ARPE-19 cells were seeded at a density of 52,000 or 32,000 cells/cm<sup>2</sup> in the wells and cultured for 24 or 48 h, respectively, followed by live-dead staining and imaging as described in Section 2.14. The cells seeded at the lower density were used for 48 h incubation to prevent reduced cell viability due to overconfluence. Positive and negative controls were included in the assay as described in Section 2.14. Image analysis was performed using images showing the interface between cells and the gel, as well as an image region showing the confluent cell monolayer. Data analysis was performed using Columbus and ImageJ as described above.

## 3. RESULTS AND DISCUSSION

### 3.1. Synthesis and Characterization of Macro CTA and Polymers

To obtain ABA triblock copolymers using RAFT polymerization, a bifunctional PEG RAFT macro CTA with a PEG molecular weight of 6 kDa was synthesized. Both terminal hydroxyl groups of PEG were coupled to the carboxylic acid groups of the RAFT CTA through Steglich esterification.<sup>20</sup> After precipitation, dialysis, and lyophilization, the macro CTA was collected as light-yellow powder with a yield of 67%. The degree of functionalization was 91–96% as determined by <sup>1</sup>H-NMR (Figure S2). GPC analysis of the PEG precursor showed an  $M_n$  of 5.3 kDa,  $M_w$  of 6.0 kDa, and dispersity ( $\bar{D}$ ) of 1.14. After conjugation of the RAFT agent, the  $M_n$  remained 5.3 kDa,  $M_w$  increased to 6.2 kDa, and  $\bar{D}$  was 1.17. GPC results for 6 kDa PEG, macro CTA, and synthesized triblock copolymers are summarized in Supporting Information, Figure S3.

RAFT polymerization was used to synthesize the triblock PNA copolymer containing PEG (P) as the midblock and thermosensitive outer blocks containing NIPAM (N) and NAS (A). Figure S4 shows the <sup>1</sup>H NMR spectrum for PNA in which the representative peaks of NIPAM and NAS are identified and used for determination of the ratio of these monomers present in the obtained polymer. The methacrylated dexamethasone prodrug (mDEX)<sup>19</sup> was synthesized and characterized (Supporting Information, Figure S5). The design of mDEX contains three important functionalities: (a) the methacrylate functionality allows polymerization of the prodrug, (b) the ester group adjacent to dexamethasone allows release of dexamethasone due to slow hydrolysis, and (c) the rate of hydrolysis can be tuned by the degree of oxidation of the thioether as described in previous work.<sup>19,27</sup> Subsequently, mDEX was used as a comonomer in the synthesis of PNADEX (Scheme 1) to obtain a polymer that slowly releases dexamethasone due to hydrolysis of the ester bond adjacent to dexamethasone. PNADEX was designed to have a similar molecular weight as PNA by reducing the NIPAM content in the feed and replacing it with mDEX. The <sup>1</sup>H NMR spectrum

of PNADEX is presented in Figure 2. The obtained copolymer composition of PNA and PNADEX matches the feed ratios of the monomer ratios in the block copolymers as determined by <sup>1</sup>H NMR (Table 1), indicating good control over the final polymer composition. Protons at positions 6, 11, and 12 were used to quantify the obtained ratio of mDEX (Figure 2), which correspond both to the dexamethasone structure (position 6) and to the methacrylated linker structure (positions 11 and 12). The ratio of the protons from the linker structures and the dexamethasone structure was approximately 1:1, indicating that the mDEX prodrug was intact after polymerization.  $M_n$  determined from <sup>1</sup>H NMR was 36.9 kDa for PNA and 37.1 kDa for PNADEX showing that the introduction of mDEX in the polymer did not affect the overall molecular weight of the polymer. The  $M_n$  values measured with GPC (16.7 kDa for PNA and 16.0 kDa for PNADEX) were lower than the  $M_n$  values determined by <sup>1</sup>H NMR which can be explained by the use of PEG as calibration standards and is in line with previous reports.<sup>28,29</sup>

The  $\bar{D}$  was 1.47 and 1.53 for PNA and PNADEX, respectively, which values were both slightly higher than previously reported values ( $\bar{D}$  1.11–1.26) for di- or triblock polymers containing NIPAM and NAS synthesized by RAFT polymerization.<sup>18,30</sup> The choice of solvent, RAFT CTA, the choice of initiator, as well as the monomer/RAFT agent and initiator/RAFT agent ratio can influence the polymerization process,<sup>31–33</sup> which in our study were chosen to be optimal for methacrylates to ensure good copolymerization of mDEX. The  $\bar{D}$  and yield of PNA compared to PNADEX hardly changed upon incorporation of mDEX, which shows that the polymerization was hardly affected by the introduction of a methacrylate monomer.

PNA had a similar CP as that of pNIPAM, 32 °C,<sup>34</sup> whereas that of PNADEX was 23 °C. The weight fraction of dexamethasone in the PNADEX polymer was 6.3%, which increased the overall hydrophobicity of the polymer. The introduction of hydrophobic dexamethasone in the thermosensitive block lowered, as expected, the CP of the triblock copolymer compared to PNA.

### 3.2. Hydrogel Characterization

PNA dissolved in PBS with or without the CA cross-linker yielded viscous solutions at 4 °C (Figure 3). For both solutions, after 3 h incubation at 37 °C, a vial tilting test showed the formation of turbid, physically cross-linked gels which retained their shape when tilting the vial. However, following incubation at 4 °C for 1 h resulted in viscous solution in the vial containing PNA without the CA cross-linker, while the hydrogel also containing CA retained its shape demonstrating the presence of chemical cross-links in the gel.

The redox sensitive nature of a hydrogel based on PNA cross-linked with CA was studied in a swelling and degradation experiment (Figure 4). The gels incubated in PBS showed some swelling during the first 2 days, as the hydrogels reached equilibrium with the aqueous environment. During the

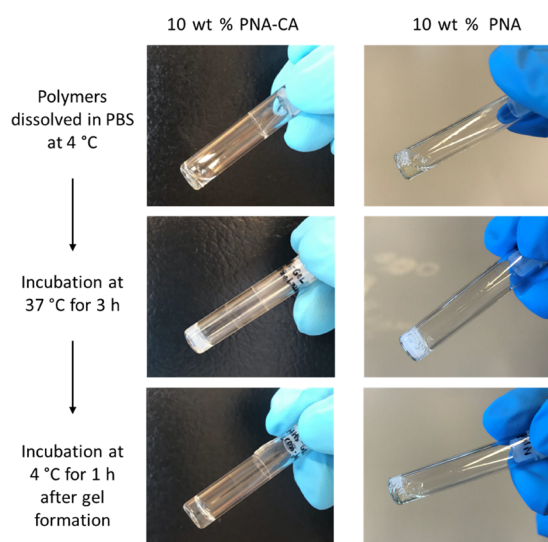


**Figure 3.** Images of vial tilting of 10 wt % PNA-CA and PNA aqueous polymer PBS solutions. First the polymers are fully dissolved in 4 °C, followed by incubation in 37 °C for 3 h. After gels were formed, the systems were incubated at 4 °C.

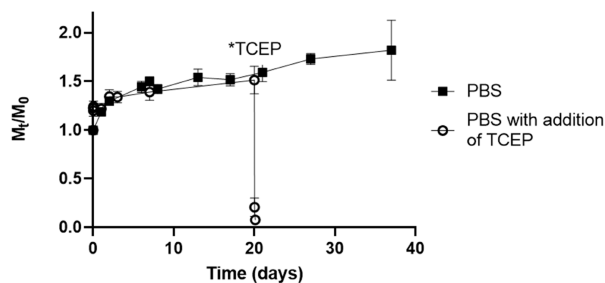


**Figure 4.** Swelling and degradation of 10 wt % PNA cross-linked with CA hydrogels ( $n = 6$ ) upon incubation in PBS at 37 °C. At day 20, TCEP was added (final concentration of 10 mM) to half of the hydrogels ( $n = 3$ ) which resulted in rapid degradation of these hydrogels.

following 38 days, the gels slightly increased in weight and reached a moderate swelling ratio of 1.7 at the end of the study at day 40. Figure 4 also shows that when at day 20, TCEP (a reducing agent) was added, the gel degraded in a few hours indicating the triggered cleavage of the disulfide bonds present in cross-links of the polymer network.

This redox sensitive nature can be utilized in making hydrogels with cross-linking that can be cleaved by the naturally existing reductive agents in the vitreous such as glutathione and thioredoxin systems,<sup>35,36</sup> resulting in a biodegradable material. However, in the vitreous environment, the possible degradation through disulfide bond cleavage is expected to be much slower than in the experimental conditions presented in this paper.

Rheological analysis was performed on samples immediately after mixing CA with PNADEX to investigate the gelation kinetics. The temperature ramp showed a cross-over of storage ( $G'$ ) and loss moduli ( $G''$ ) at 27 °C indicating thermogelation (Figure 5A). At the end of the temperature ramp at 37 °C,  $G'$  and  $G''$  were 138 and 29 Pa, respectively. The  $G'$  remained higher than  $G''$  while the gel was cooled down demonstrating the formation of a covalently cross-linked polymer network. The covalent cross-linking is likely accelerated at elevated

temperatures due to the fact that the NHS functional groups are in close proximity above the LCST due to the self-assembly of the thermosensitive blocks of the polymers. Upon cooling to temperatures below the CP, the hydrogel stiffness increased even further, likely due to the relaxation of the polymer chains because of hydration of pNIPAM, exposing the yet unreacted functional moieties resulting in further cross-links. At the end of the cooling ramp at 4 °C, the  $G'$  and  $G''$  were 519 and 191 Pa, respectively.

The PNADEX-CA hydrogel showed linear viscoelastic behavior up to 100% strain (Supporting Information, Figure S6A). Oscillation strain of 800% was chosen for the strain and recovery experiment (Figure 5B) to investigate possible self-healing properties of the hydrogel. First, the hydrogel was allowed to form in a rheometer followed by increasing the strain to 800% for 2 min to compromise the network integrity (indicated by  $\Delta$  in Figure 5B), after which the hydrogel was allowed to recover at a strain of 0.1% for 20 min. In the repeated strain cycles, we observed rapid recovery of the  $G'$  and  $G''$  values close to the initial values at low strains, indicating the network's self-healing properties.

To get mechanistic insight into the role of the disulfide bonds in the self-healing properties of the network, hydrogels cross-linked with hexamethylenediamine, which has a similar structure to CA but lacks the disulfide bridge, were prepared. The rheological characterization of the 10 wt % PNADEX-hexamethylenediamine hydrogel (Figure 5C,D) showed similar physical and chemical cross-linking behavior and a linear viscoelastic regime as the PNADEX-CA hydrogel. However, the moduli at the end of the temperature ramp at 37 °C were significantly higher with the hydrogel cross-linked with hexamethylenediamine than with the hydrogel cross-linked by CA;  $G'$  and  $G''$  were 394 and 56 Pa, respectively. Likewise, after cooling down the hydrogel cross-linked by hexamethylenediamine to 4 °C, the  $G'$  and  $G''$  were 844 and 261 Pa, respectively, which were significantly higher than for the hydrogel cross-linked by CA ( $G'$  and  $G''$  of 519 and 191 Pa, respectively). The lower moduli of the hydrogel cross-linked by CA can likely be explained by the dynamic disulfide exchange (as schematically shown in Figure 1B). The strain and recovery experiment of the hydrogel cross-linked by hexamethylenediamine showed that upon removing the mechanical stress, the  $G'$  and  $G''$  were significantly lower as compared to the initial state, and the strength of the hydrogel slightly decreased further over repeated strain and recovery cycles (Figure 5D). This observation supports the contribution of the disulfide bonds in self-healing properties of the PNADEX-CA hydrogels.

Importantly, the 10 wt % PNADEX-CA hydrogel was easily injectable through a 30G needle likely due to the exchange of disulfide bonds resulting in shear-thinning properties (Figure 6). The injected gel strands retained their integrity and reshaped post-injection into different shapes (globular and linear) due to the self-healing properties of the material. However, this behavior was not observed for the hydrogel cross-linked with hexamethylenediamine, which was therefore not injectable. The injectability of the CA cross-linked hydrogel is crucial for use as the intravitreal drug delivery system. Important to mention is the relatively small injection volume needed for this formulation ( $\sim 90 \mu\text{L}$ ) compared to the total of 4.6 mL of human vitreous.<sup>37</sup> This small volume of the turbid hydrogel could be injected outside of the line of sight or



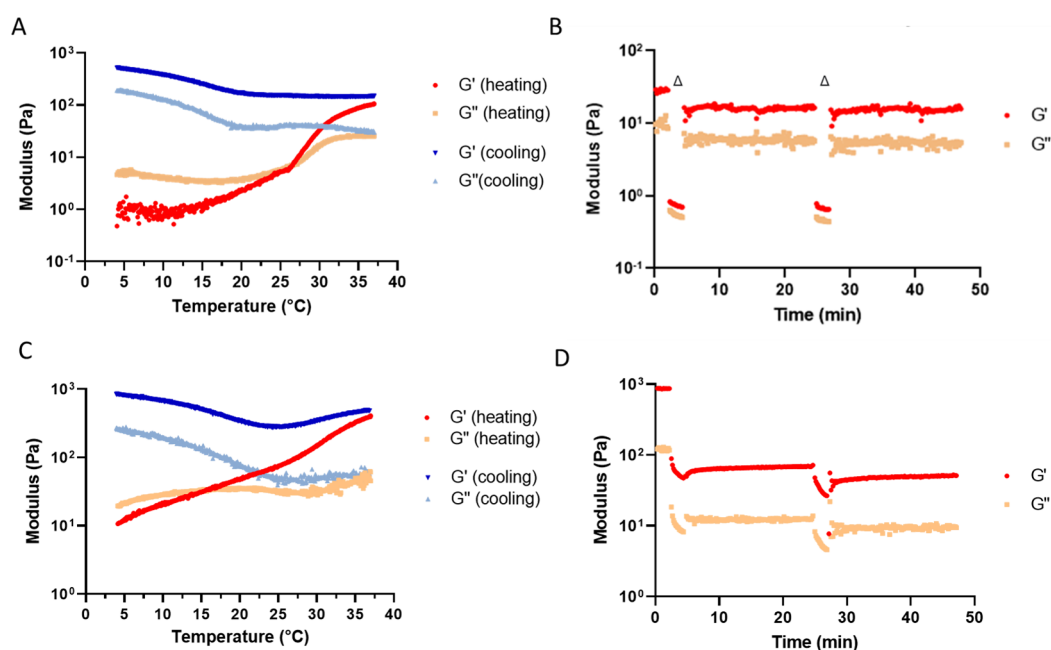


**Figure 5.** (A) Rheological behavior of the 10 wt % PNADEX-CA hydrogel. Temperature ramp showing  $G'$  and  $G''$  changes upon physical and chemical cross-linking. (B) Repeated strain-recovery cycles showed recovery of the PNADEX-CA hydrogel after applied strain ( $\Delta$ , 800% strain for 2 min) was reduced (0.1% strain). (C) Rheological characterization of the PNADEX hydrogel cross-linked with hexamethylenediamine. Temperature ramp showing  $G'$  and  $G''$  changes upon physical and chemical cross-linking. (D) Repeated strain-recovery cycles showed that the PNADEX-hexamethylenediamine hydrogel was unable to recover after the applied strain ( $\Delta$ ) was reduced, indicating that the hydrogel lacks self-healing properties.

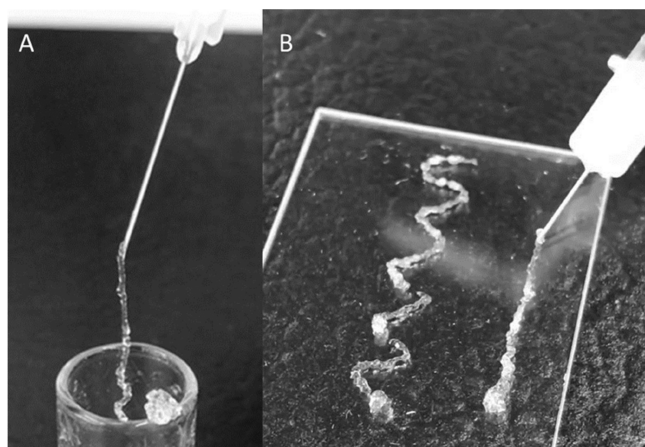


**Figure 6.** Injectability of the 10 wt % PNADEX-CA hydrogel at room temperature through a 30G needle. Gel strands retained their shape after injection and could be shaped into a globular structure (A) or various linear shapes (B).

below the visual axis to prevent any disturbances to vision similar to that currently done for intraocular implants.

### 3.3. Release of Dexamethasone from the Hydrogel

PNADEX-CA hydrogels (approximately 100 mg, 10 wt %,  $n = 3$ ) were prepared and contained on average  $623 \pm 32 \mu\text{g}$  of dexamethasone, which was determined based on the  $^1\text{H}$  NMR spectrum of the polymer (Section 3.1) and the mass of the polymeric solution used for each hydrogel. The cleavage of dexamethasone from the mDEX prodrug through hydrolysis was shown to be pH-dependent and followed pseudo-first-order kinetics in the aqueous medium (Supporting Information, Figure S7), which is in line with the previous experimental data regarding polymeric particles loaded with

dexamethasone prodrugs with sulfide ester-based linkers with different degrees of oxidation.<sup>19</sup> The slowest hydrolyzing linker was chosen for development of a hydrogel that was aimed to release dexamethasone for months. Indeed, Figure 7A shows that dexamethasone was released from the hydrogel in a buffered aqueous medium for more than 400 days. The release was fitted to a first-order model (Figure 7B), using the following equation:  $\ln(M_t) = -k \cdot t + \ln(M_0)$  (where  $M_t$  is the amount of dexamethasone still coupled to the hydrogel at time  $t$ ,  $k$  is the release constant, and  $M_0$  is the amount of dexamethasone coupled at time 0), which gave a  $k$  value of  $0.0017 \text{ d}^{-1}$  with  $R^2 = 0.91$ , corresponding to a half-life of 408 days.

Noteworthy, the release of dexamethasone from the free mDEX at pH 7.4 was faster than from the hydrogel ( $t_{1/2}$  5.9 and 408 days, respectively) which points to slower hydrolysis of ester bonds between dexamethasone and the polymer backbone, likely due to lower water activity in the hydrophobic domains of the hydrogel<sup>38,39</sup> compared to mDEX dissolved in the aqueous medium. As an example, the hydrogel released on an average of  $1.35 \pm 0.04 \mu\text{g}/\text{day}$  at 100 days of release (Figure 7C). As a consequence of the first-order hydrolysis kinetics, the released amount per time unit gradually decreased over time. However, at the end of the study (day 430), the gel still released  $0.37 \pm 0.10 \mu\text{g}$  of dexamethasone/day.

The concentration of dexamethasone in the vitreous compartment for 500 days after injection of 100 mg of 10 wt % PNADEX-CA hydrogel was simulated as described in Section 2.11. The compartmental model consists of the amount of dexamethasone released per day from the hydrogel based on in vitro release kinetics and elimination kinetics of dexamethasone from the vitreous based on values reported in the literature (Table S1). Figure 8A shows the simulated concentration of dexamethasone after administration of the

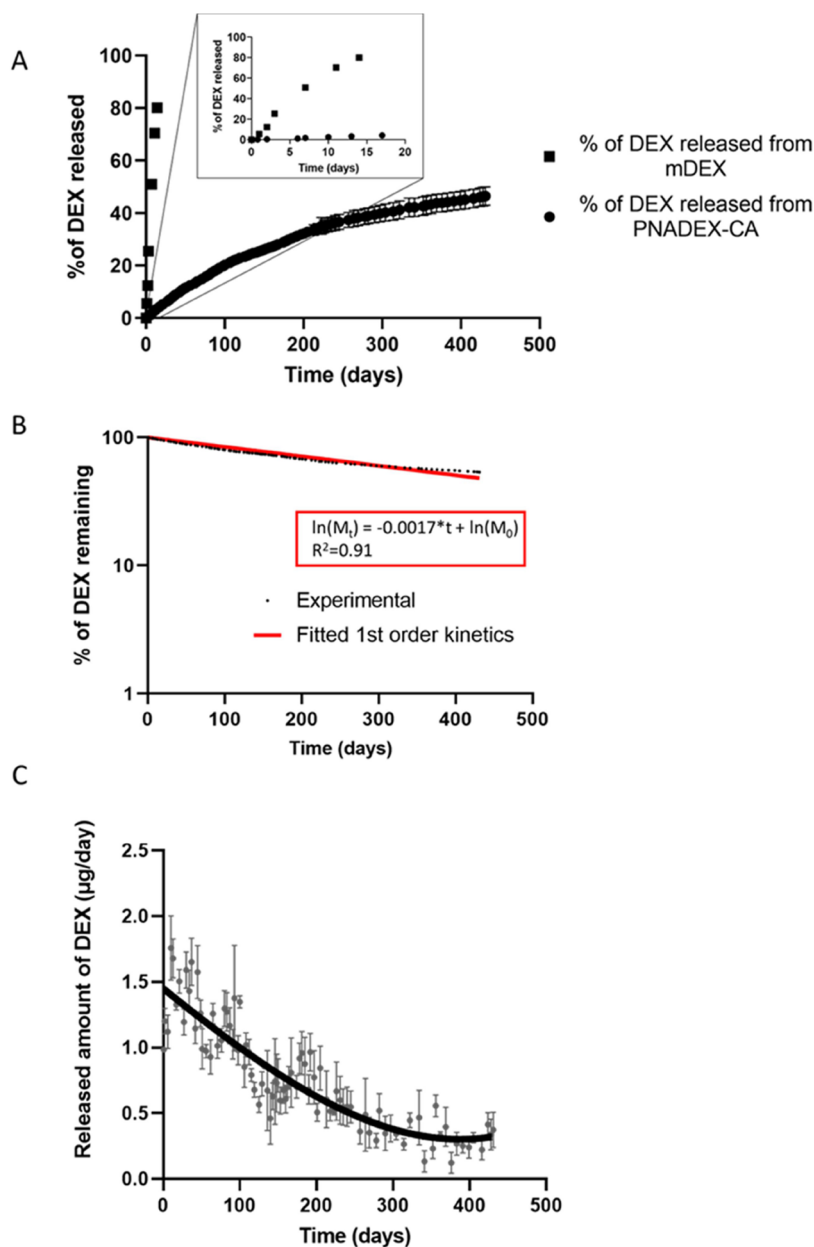


**Figure 7.** (A) In vitro release of dexamethasone from the 10 wt % PNADEX-CA hydrogel and mDEX. (B) Curve fitting of dexamethasone release from the PNADEX-CA hydrogel. (C) Average released amount of dexamethasone/day is calculated as a first derivative between consecutive time points in panel A and the curve is fitted using a nonlinear model.

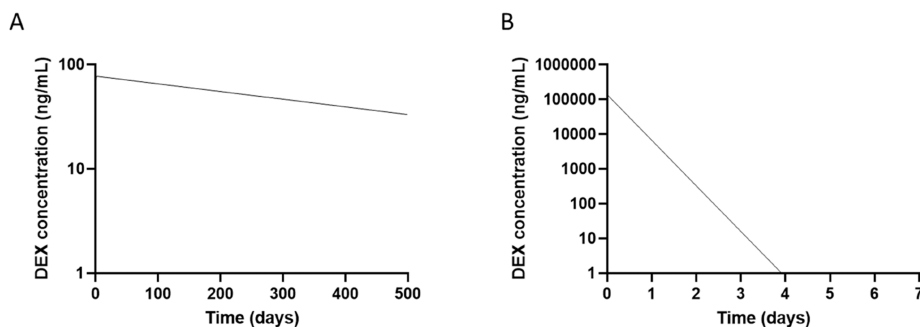


**Figure 8.** Simulated vitreal concentration of dexamethasone after administration of 100 mg of 10 wt % PNADEX-CA hydrogel (90  $\mu\text{L}$ ) in the human vitreous (A) and bolus injection of solution with the same dose of dexamethasone (623  $\mu\text{g}$ ) (B) using the compartmental STELLA model.

hydrogel in the human vitreous. Maximum concentration ( $C_{\text{max}}$ ) of 77 ng/mL is achieved 2.5 days post-injection, and the

concentrations gradually drop to 33 ng/mL at day 500. For comparison, the dexamethasone concentration in the vitreous

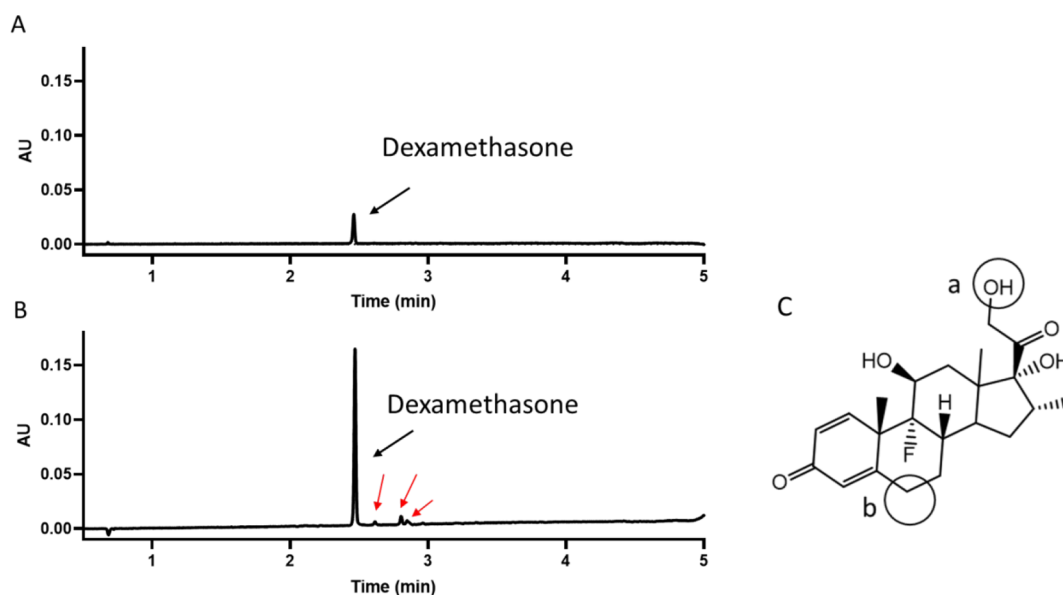


**Figure 9.** UPLC chromatograms of release the sample taken at 2 (A) and 79 days (B) after the start of the experiment. The black arrow indicates dexamethasone, whereas the red arrows are degradation products identified as modified dexamethasone. (C) Chemical modification of dexamethasone in the aqueous medium is proposed to occur at the hydroxyl group (a) and the circled ring structure (b).<sup>41</sup>

after a bolus injection of dexamethasone solution (same dose as for the hydrogel formulation) was simulated. Figure 8B shows that the  $C_{\max}$  was 138,000 ng/mL immediately after injection of this solution. Already after 4 days of administration, most of the drug has been eliminated, with the concentration in the vitreous being below 1 ng/mL. These simulations highlight the potential of the hydrogel to significantly prolong the concentration of dexamethasone after its intravitreal administration.

In clinical use, the maximum volume for intravitreal injection in humans is 100  $\mu\text{L}$ <sup>6</sup> and since intravitreally administered dexamethasone is efficacious in the nanomolar range,<sup>40</sup> the simulations showed that the vitreal dexamethasone concentration after intravitreal administration of 100 mg of 10 wt % PNADEX-CA hydrogel is sufficient for maintaining the therapeutic range in the vitreous for at least 500 days. This makes the PNADEX-CA hydrogel formulation a potential alternative to the currently clinically available sustained release system for ocular drug delivery of dexamethasone, the Ozurdex implant. This drug delivery system is based on PLGA and loaded with 700 mg of dexamethasone<sup>7</sup> (which is close to the used dose, 623 mg, in this study). Studies of Ozurdex in cynomolgus monkeys showed a peak dexamethasone concentration ( $C_{\max}$ ) of  $213 \pm 49$  ng/mL in the vitreous at 60 days post-treatment.<sup>40</sup> However, between 90 and 180 days, the dexamethasone release rate decreased and resulted in vitreal concentrations of  $0.00131 \pm 0.0002$  ng/mL at day 180. As a comparison, the simulated vitreal concentrations for the here reported hydrogel formulation at 60, 90, and 180 days after administration in humans are 70, 68, and 57 ng/mL, respectively. Although the simulated  $C_{\max}$  of dexamethasone for our hydrogel formulation is lower than that for the Ozurdex implant, it is still well within the therapeutic range, and importantly, the released amounts from the hydrogel at later time points clearly outperform those of the implant formulation.

Dexamethasone has limited stability in the aqueous medium with several byproducts being formed over time.<sup>41</sup> Therefore,

the integrity of the released dexamethasone from the hydrogel and mDEX was studied using UPLC and LC–MS analysis. Only minor degradation products were observed in the UPLC chromatograms of the release samples even after 79 days of release (Figure 9A,B). A previous study showed that chemical modifications of dexamethasone in PBS occur both at a hydroxyl group or at one of the ring structures of dexamethasone, as indicated in Figure 9C.<sup>41</sup> However, as this hydroxyl group of dexamethasone is coupled to the hydrogel network via the methacrylated linker, the drug is only susceptible to degradation by this route after cleavage and release from the hydrogel network. Nevertheless, modifications in the ring structure could potentially occur when dexamethasone is coupled to the hydrogel. LC–MS analysis was carried out to (a) confirm the formation of native dexamethasone from mDEX after hydrolysis of the ester bond adjacent to dexamethasone in the linker and (b) to identify dexamethasone degradation products detectable in the UPLC chromatogram. Indeed, LC–MS analysis showed that essentially native dexamethasone was released from mDEX (Supporting Information, Figure S9). Based on the degradation products of dexamethasone identified by LC–MS (Supporting Information, Figure S10) and comparing the corresponding peaks in chromatograms of the PNADEX-CA hydrogel release samples, small fractions of modified dexamethasone were identified in the release samples (Supporting Information, Figure S11). The dexamethasone degradation products identified were all modifications to the hydroxyl group with ring structures intact.

### 3.4. Cytocompatibility of the Polymers and the Cross-Linker

The cytocompatibility of PNADEX and CA was evaluated in the ARPE-19 retinal cell line which originates from the eye and is well characterized<sup>42,43</sup> using two different methods.

First, we used the alamarBlue assay that measures the metabolic activity of cells to evaluate the cell viability exposed to series dilutions of PNADEX and CA in the culture medium (Figure 10). This figure shows that PNADEX did not reduce



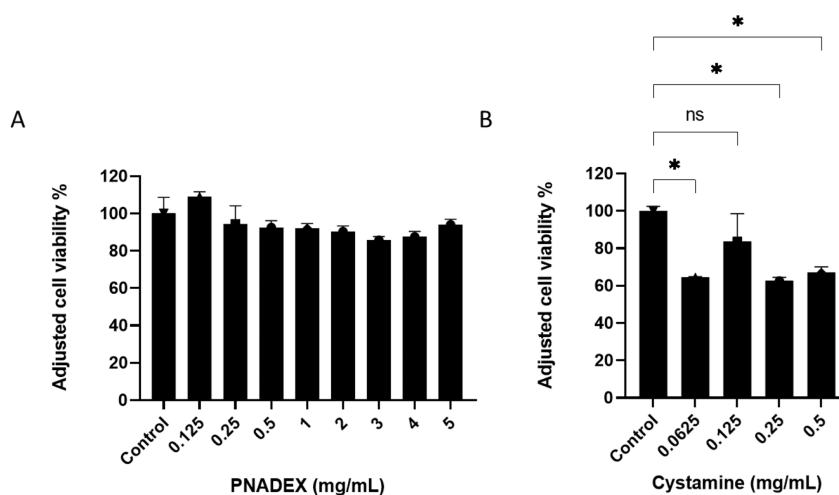


**Figure 10.** AlamarBlue assay of ARPE-19 cells after incubation for 24 h at 37 °C with series dilutions of PNADEX (A) and CA (B). The cell viability is adjusted to 100% for the control cells incubated with the normal cell culture medium. The ANOVA analysis showed that PNADEX was well tolerated by the cells at all the tested concentrations ( $p > 0.05$ ), whereas the cell viability was significantly reduced ( $p < 0.05$ ) at CA concentrations 0.5, 0.25, and 0.0625 mg/mL compared to untreated control cells.

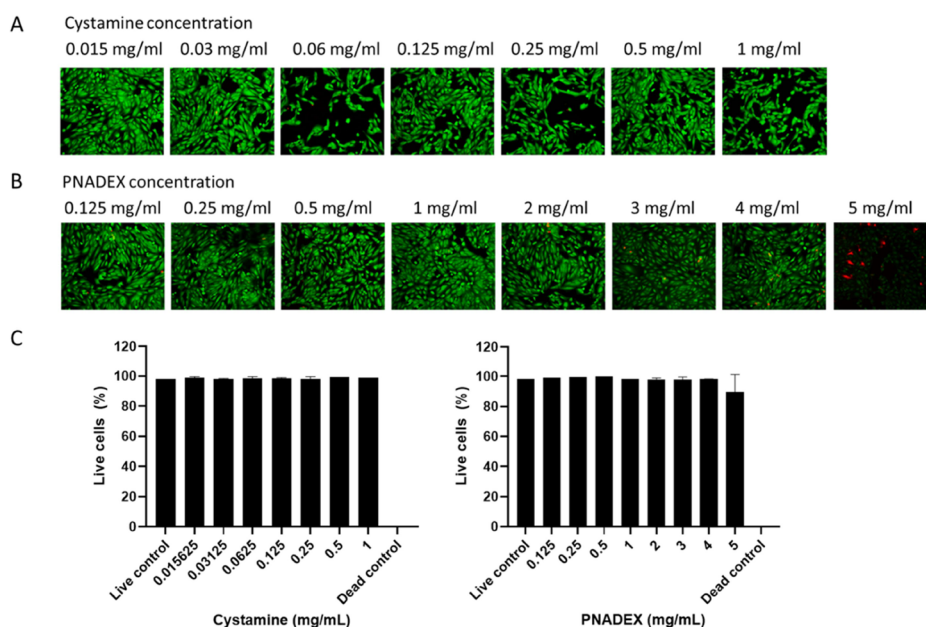


**Figure 11.** Live-dead assay of ARPE-19 cells exposed to PNADEX and cystamine. Living cells are stained green and dead cells are stained red. (A) Evaluation of cystamine in ARPE-19. (B) Evaluation of PNADEX in ARPE-19. Lower green signal intensity can be seen at the higher polymer concentration due to the turbidity of the cell culture medium. (C) Results of live-dead assay for cystamine and PNADEX. The live control of cells was incubated in normal cell culture media, and the dead control of cells was incubated with 1% Triton X-100.

cell viability (with significance level  $> 0.05$ ) compared to untreated control cells, at any of the tested concentrations (up to 5 mg/mL) whereas CA reduced the viability of ARPE-19 cells to 64% already at the lowest tested concentration (0.0625 mg/mL). The cell viability was significantly reduced ( $p < 0.05$ ) at all the other CA concentrations tested apart from 0.125 mg/mL, which reduced the cell viability only to 84%. However, the CA concentrations are expected to be much lower in a clinical setting (for example, in case 10% of free cross-linker would remain unreacted in a 100 mg of injection of the hydrogel into the vitreous of 4.6 ml<sup>37</sup>, the expected total load of CA would only be 0.01 mg/mL).

The cytocompatibility of the materials was also evaluated using a live-dead dual staining (Figure 11). This figure shows

that CA did not show cell toxicity in ARPE-19 cells at the concentrations studied (cell viability 97–99%). Moreover, PNADEX was also well tolerated by ARPE-19 cells at the concentrations tested (cell viability 90–100%), indicating good cytocompatibility of PNADEX. The signal intensity of Calcein AM and PI slightly decreased at the highest concentration (5 mg/mL) of PNADEX due to the turbidity caused by the polymer in the cell culture medium (Figure 11B). However, when enhancing the brightness of the image, it is evident that majority of the cells in the well were stained green (Supporting Information, Figure S12).

The cytotoxicity of the PNADEX-CA hydrogel on a growing monolayer of ARPE-19 cells was studied to investigate whether the hydrogel or the NHS byproduct of cross-linking possibly

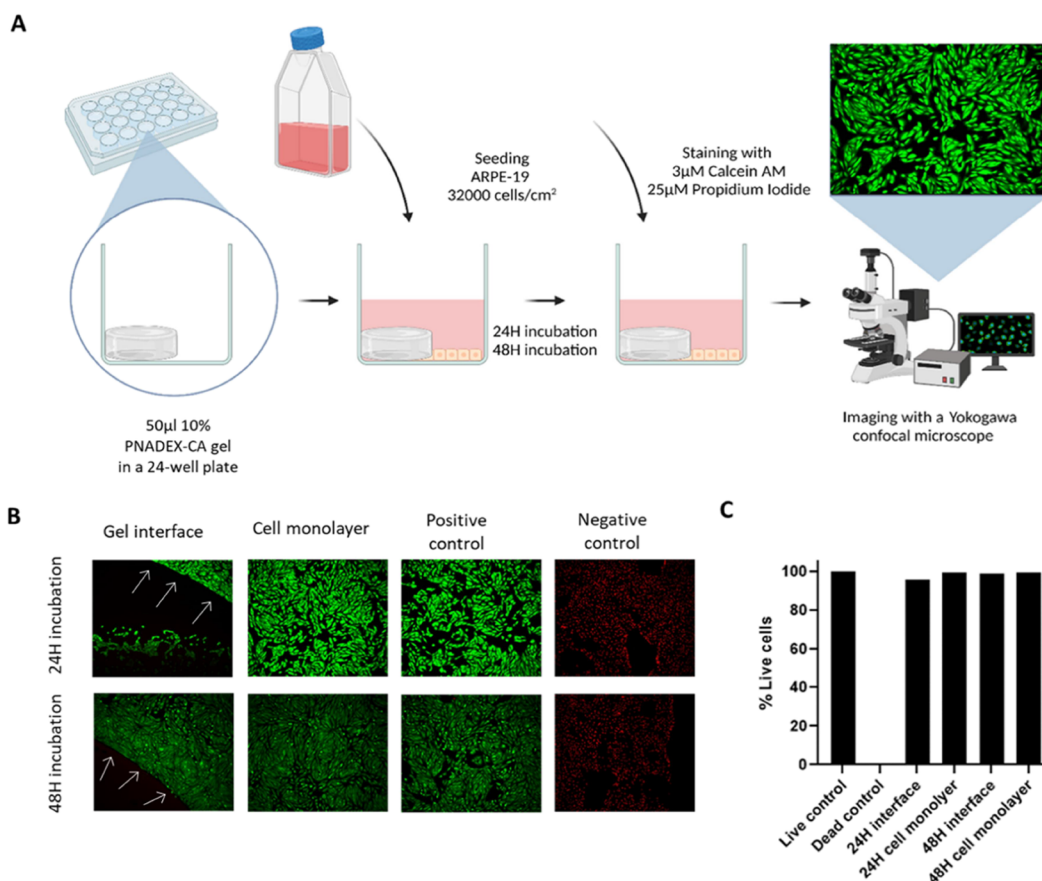


**Figure 12.** (A) Culturing of ARPE-19 cells in the presence of the 10 wt % PNADEX hydrogel. The hydrogel was formed on the plate covering 1/3 of the surface of the well. ARPE-19 cells were seeded on the top and around the hydrogel and allowed to attach and grow for 24 and 48 h at 37 °C, after which they were stained with Calcein AM and PI and imaged with a confocal microscope ( $n = 1$  for each condition). The image is made with BioRender.com. (B) Images of the cells at the gel interface and the cell monolayer after 24 and 48 h of incubation. The white arrows indicate the edge of the gel layer. Slight differences in the signal intensity were observed between 24 and 48 h incubation due to the day-to-day variation in staining. (C) Cell viability of ARPE-19 cultured in the presence of the 10 wt % PNADEX-CA hydrogel. The live control of cells was incubated in normal cell culture media, and the dead control of cells was incubated with 1% Triton X-100.

compromises the cell viability. PNADEX-CA hydrogels were formed directly in a well of a 24-well plate (Figure 12A), followed by seeding the ARPE-19 cells. Figure 12B shows that the cells did not attach well to the hydrogel; however, the cells grew abundantly close to the gel interface. Live-dead staining was used to determine the viability of the cells growing in the near proximity of the gel edge and in the cell monolayer. Only few individual dead cells were found at the gel–monolayer interface after 24 h of incubation. Moreover, the viability was comparable to the positive control at both time points in all parts of the well, indicating that the gel is well tolerated by the cells (Figure 12C).

#### 4. CONCLUSIONS

In this study, we investigated the suitability of a thermosensitive hydrogel made of the ABA triblock copolymer PNADEX for long-term release of dexamethasone. The self-healing properties enabled the hydrogel to be injectable through a 30G needle, making its intraocular administration possible. Release of dexamethasone in vitro was achieved for more than a year, which highlights the potential of this delivery system for treating chronic ocular inflammatory diseases. Importantly, the release of dexamethasone was achieved with minimal formation of degradation products, which, given limited aqueous stability of dexamethasone over an extended period

of time, emphasizes the capacity of the hydrogel to protect the drug from chemical modifications prior release. Finally, both PNADEX and the hydrogel based on this polymer were well tolerated in vitro, which combined with the long release profile and injectable nature of the hydrogel, making this formulation an attractive candidate for further preclinical testing for treatment of ocular inflammatory diseases.

#### ■ ASSOCIATED CONTENT

##### Supporting Information

The Supporting Information is available free of charge at <https://pubs.acs.org/doi/10.1021/acspolymersau.2c00038>.

Additional experimental details, materials, methods, and synthesis schemes; description of the pharmacokinetic simulation model and parameters; cell culture imaging settings, <sup>1</sup>H NMR spectra for RAFT macro CTA, polymers, and monomers; and GPC data, prodrug characterization, rheology data, stability of the prodrug and the drug in an aqueous medium, LC–MS analysis of the released drug and identification of degradation products, and additional cytotoxicity figure (PDF)

## AUTHOR INFORMATION

### Corresponding Author

**Tina Vermonden** – Department of Pharmaceutics, Utrecht Institute for Pharmaceutical Sciences, Faculty of Science, Utrecht University, Utrecht 3584 CG, The Netherlands; [orcid.org/0000-0002-6047-5900](https://orcid.org/0000-0002-6047-5900); Email: [t.vermonden@uu.nl](mailto:t.vermonden@uu.nl)

### Authors

**Ada Annala** – Department of Pharmaceutics, Utrecht Institute for Pharmaceutical Sciences, Faculty of Science, Utrecht University, Utrecht 3584 CG, The Netherlands

**Blessing C. Ilochonwu** – Department of Pharmaceutics, Utrecht Institute for Pharmaceutical Sciences, Faculty of Science, Utrecht University, Utrecht 3584 CG, The Netherlands

**Danny Wilbie** – Department of Pharmaceutics, Utrecht Institute for Pharmaceutical Sciences, Faculty of Science, Utrecht University, Utrecht 3584 CG, The Netherlands

**Amir Sadeghi** – School of Pharmacy, University of Eastern Finland, Kuopio 70210, Finland

**Wim E. Hennink** – Department of Pharmaceutics, Utrecht Institute for Pharmaceutical Sciences, Faculty of Science, Utrecht University, Utrecht 3584 CG, The Netherlands; [orcid.org/0000-0002-5750-714X](https://orcid.org/0000-0002-5750-714X)

Complete contact information is available at: <https://pubs.acs.org/10.1021/acspolymersau.2c00038>

### Author Contributions

CRedit: **Ada Annala** conceptualization (equal), data curation (equal), formal analysis (equal), investigation (lead), methodology (lead), validation (equal), writing-original draft (equal), writing-review & editing (equal); **Blessing C. Ilochonwu** investigation (equal), methodology (equal); **Danny Wilbie** investigation (equal), visualization (equal), writing-original draft (supporting); **Amir Sadeghi** data curation (equal), software (equal), writing-original draft (supporting); **Wim E. Hennink** funding acquisition (equal), supervision (equal), writing-review & editing (equal); **Tina Vermonden** funding acquisition (equal), project administration (equal), supervision (equal), writing-review & editing (equal).

### Notes

The authors declare no competing financial interest.

## ACKNOWLEDGMENTS

This project has received funding from the European Union's Horizon 2020 research and innovation program under the Marie Skłodowska-Curie grant agreement No 722717. The authors acknowledge R.A. de Kort for assistance with curve fitting in Python and Vito Thijssen for assistance with the LC-MS experiments.

## REFERENCES

- del Amo, E. M.; Rimpelä, A. K.; Heikkinen, E.; et al. Pharmacokinetic aspects of retinal drug delivery. *Prog. Retin. Eye Res.* **2017**, *57*, 134–185.
- Delplace, V.; Payne, S.; Shoichet, M. Delivery strategies for treatment of age-related ocular diseases: From a biological understanding to biomaterial solutions. *J. Controlled Release* **2015**, *219*, 652–668.
- Gaballa, S. A.; Kompella, U. B.; Elgarhy, O.; et al. Corticosteroids in ophthalmology: drug delivery innovations, pharmacology, clinical applications, and future perspectives. *Drug Deliv. Transl. Res.* **2021**, *11*, 866–893.
- Abadia, B.; Calvo, P.; Ferreras, A.; Bartol, F.; Verdes, G.; Pablo, L. Clinical Applications of Dexamethasone for Aged Eyes. *Drugs Aging* **2016**, *33*, 639–646.
- Cáceres-Del-Carpio, J.; Costa, R. D.; Haider, A.; Narayanan, R.; Kuppermann, B. D. Corticosteroids: Triamcinolone, dexamethasone and fluocinolone. *Dev. Ophthalmol.* **2016**, *55*, 221–231.
- Grzybowski, A.; Told, R.; Sacu, S.; et al. 2018 Update on Intravitreal Injections: Euretina Expert Consensus Recommendations. *Ophthalmologica* **2018**, *239*, 181–193.
- Allergan Inc. Ozurdex Package insert. 2009. <https://allergan-web-cdn-prod.azureedge.net/allerganindia/allerganindia/media/allergan-india/products/ozurdexpackinsert.pdf>. Accessed September 3, 2021.
- Gao, Y.; Sun, Y.; Ren, F.; Gao, S. PLGA-PEG-PLGA hydrogel for ocular drug delivery of dexamethasone acetate. *Drug Dev. Ind. Pharm.* **2010**, *36*, 1131–1138.
- Kicková, E.; Salmaso, S.; Mastrotto, F.; Caliceti, P.; Urtti, A. Pullulan based bioconjugates for ocular dexamethasone delivery. *Pharmaceutics* **2021**, *13*, 791.
- London, N. J. S.; Chiang, A.; Haller, J. A. The dexamethasone drug delivery system: Indications and evidence. *Adv. Ther.* **2011**, *28*, 351–366.
- Zhang, L.; Shen, W.; Luan, J.; et al. Sustained intravitreal delivery of dexamethasone using an injectable and biodegradable thermogel. *Acta Biomater.* **2015**, *23*, 271–281.
- Ilochonwu, B. C.; Urtti, A.; Hennink, W. E.; Vermonden, T. Intravitreal hydrogels for sustained release of therapeutic proteins. *J. Controlled Release* **2020**, *326*, 419–441.
- Uman, S.; Dhand, A.; Burdick, J. A. Recent advances in shear-thinning and self-healing hydrogels for biomedical applications. *J. Appl. Polym. Sci.* **2020**, *137*, 48668.
- Bertsch, P.; Diba, M.; Mooney, D. J.; Leeuwenburgh, S. C. G. Self-Healing Injectable Hydrogels for Tissue Regeneration. *Chem. Rev.* **2022**, No. c00179.
- Yang, W. J.; Tao, X.; Zhao, T.; Weng, L.; Kang, E. T.; Wang, L. Antifouling and antibacterial hydrogel coatings with self-healing properties based on a dynamic disulfide exchange reaction. *Polym. Chem.* **2015**, *6*, 7027–7035.
- Wu, L.; Di Cio, S.; Azevedo, H. S.; Gautrot, J. E. Photoconfigurable, Cell-Remodelable Disulfide Cross-linked Hyaluronic Acid Hydrogels. *Biomacromolecules* **2020**, *21*, 4663–4672.
- Wen, J.; Jia, Z.; Zhang, X.; Pan, M.; Yuan, J.; Zhu, L. Tough, thermo-Responsive, biodegradable and fast self-healing polyurethane hydrogel based on microdomain-closed dynamic bonds design. *Mater. Today Commun.* **2020**, *25*, No. 101569.
- Zhang, J.; Jiang, X.; Zhang, Y.; Li, Y.; Liu, S. Facile fabrication of reversible core cross-linked micelles possessing thermosensitive swellability. *Macromolecules* **2007**, *40*, 9125–9132.
- Crielaard, B. J.; Rijcken, C. J. F.; Quan, L.; van der Wal, S.; Altintas, I.; van der Pot, M.; Kruijtzter, J. A. W.; Liskamp, R. M. J.; Schiffelers, R. M.; van Nostrum, C. F.; Hennink, W. E.; Wang, D.; Lammers, T.; Storm, G. Glucocorticoid-loaded core-cross-linked polymeric micelles with tailorable release kinetics for targeted therapy of rheumatoid arthritis. *Angew. Chem. Int. Ed.* **2012**, *124*, 7366–7370.
- Neises, B.; Steglich, W. Simple Method for the Esterification of Carboxylic Acids. *Angew. Chem. Int. Ed.* **1978**, *17*, 522–524.
- Fliervoet, L. A. L.; Lisitsyna, E. S.; Durandin, N. A.; Kotsis, I.; Maas-Bakker, R. F. M.; Yliperttula, M.; Hennink, W. E.; Vuorimaa-Laukkanen, E.; Vermonden, T. Structure and Dynamics of Thermosensitive pDNA Polyplexes Studied by Time-Resolved Fluorescence Spectroscopy. *Biomacromolecules* **2020**, *21*, 73.
- Postma, A.; Davis, T. P.; Donovan, A. R.; Li, G.; Moad, G.; Mulder, R.; O'Shea, M. S. A simple method for determining protic end-groups of synthetic polymers by <sup>1</sup>H NMR spectroscopy. *Polymer* **2006**, *47*, 1899–1911.
- Neradovic, D.; Hinrichs, W. L. J.; Kettenes-van Den Bosch, J. J.; Hennink, W. E. Poly(N-isopropylacrylamide) with hydrolyzable lactic



acid ester side groups: A new type of thermosensitive polymer. *Macromol. Rapid Commun.* **1999**, *20*, 577–581.

(24) Virtanen, P.; Gommers, R.; Oliphant, T. E.; et al. SciPy 1.0: fundamental algorithms for scientific computing in Python. *Nat. Methods* **2020**, *17*, 261–272.

(25) Kicková, E.; Sadeghi, A.; Puranen, J.; Tavakoli, S.; Sen, M.; Ranta, V. P.; Arango-Gonzalez, B.; Bolz, S.; Ueffing, M.; Salmaso, S.; Caliceti, P.; Toropainen, E.; Ruponen, M.; Urtti, A. Pharmacokinetics of pullulan–dexamethasone conjugates in retinal drug delivery. *Pharmaceutics* **2021**, *14*, 12.

(26) Sadeghi, A.; Ruponen, M.; Puranen, J.; et al. Imaging, quantitation and kinetic modelling of intravitreal nanomaterials. *Int. J. Pharm.* **2022**, *621*, No. 121800.

(27) Coimbra, M.; Rijcken, C. J. F.; Stigter, M.; Hennink, W. E.; Storm, G.; Schifflers, R. M. Antitumor efficacy of dexamethasone-loaded core-crosslinked polymeric micelles. *J. Controlled Release* **2012**, *163*, 361–367.

(28) Wang, Y.; van Steenberg, M. J.; Beztinna, N.; Shi, Y.; Lammers, T.; van Nostrum, C. F.; Hennink, W. E. Biotin-decorated all-HPMA polymeric micelles for paclitaxel delivery. *J. Controlled Release* **2020**, *328*, 970–984.

(29) Najafi, M.; Kordalivand, N.; Moradi, M. A.; et al. Native Chemical Ligation for Cross-Linking of Flower-Like Micelles. *Biomacromolecules* **2018**, *19*, 3766–3775.

(30) Li, Y.; Lokitz, B. S.; McCormick, C. L. RAFT synthesis of a thermally responsive ABC triblock copolymer incorporating N-acryloxysuccinimide for facile in situ formation of shell cross-linked micelles in aqueous media. *Macromolecules* **2006**, *39*, 81–89.

(31) Favier, A.; Charreyre, M. T. Experimental requirements for an efficient control of free-radical polymerizations via the reversible addition-fragmentation chain transfer (RAFT) process. *Macromol. Rapid Commun.* **2006**, *27*, 653–692.

(32) Gujraty, K. V.; Yanjarappa, M. J.; Saraph, A.; Joshi, A.; Mogridge, J.; Kane, R. S. Synthesis of Homopolymers and Copolymers Containing an Active Ester of Acrylic Acid by RAFT: Scaffolds for Controlling Polyvalent Ligand Display. *J. Polym. Sci., Part A: Polym. Chem.* **2008**, *46*, 7246.

(33) Moad, G.; Rizzardo, E.; Thang, S. H. Living radical polymerization by the RAFT process A second update. *Aust. J. Chem.* **2009**, *62*, 1402–1472.

(34) Najafi, M.; Hebels, E.; Hennink, W. E.; Vermonden, T. Poly(*N*-isopropylacrylamide): Physicochemical Properties and Biomedical Applications. In *Temperature-Responsive Polymers*; Wiley: 2018; pp 1–34.

(35) Santos, F. M.; Mesquita, J.; Castro-De-sousa, J. P.; Ciordia, S.; Paradela, A.; Tomaz, C. T. Vitreous Humor Proteome: Targeting Oxidative Stress, Inflammation, and Neurodegeneration in Vitreoretinal Diseases. *Antioxidants* **2022**, *11*, 505.

(36) Murthy, K. R.; Goel, R.; Subbannayya, Y.; et al. Proteomic analysis of human vitreous humor. *Clin. Proteomics* **2014**, *11*, 29.

(37) Azhdam, A. M.; Goldberg, R. A.; Ugradar, S. In vivo measurement of the human vitreous chamber volume using computed tomography imaging of 100 eyes. *Transl. Vis. Sci. Technol.* **2020**, *9*, 2.

(38) Yoshioka, S.; Aso, Y.; Terao, T. Effect of Water Mobility on Drug Hydrolysis Rates in Gelatin Gels. *Pharm. Res.* **1992**, *9*, 607–612.

(39) Mikac, U.; Sepe, A.; Gradišek, A.; Kristl, J.; Apih, T. Dynamics of water and xanthan chains in hydrogels studied by NMR relaxometry and their influence on drug release. *Int. J. Pharm.* **2019**, *563*, 373–383.

(40) Chang-Lin, J. E.; Attar, M.; Acheampong, A. A.; Robinson, M. R.; Whitcup, S. M.; Kuppermann, B. D.; Welty, D. Pharmacokinetics and pharmacodynamics of a sustained-release dexamethasone intravitreal implant. *Investig. Ophthalmol. Vis. Sci.* **2011**, *52*, 80–86.

(41) Matter, B.; Ghaffari, A.; Bourne, D.; Wang, Y.; Choi, S.; Kompella, U. B. Dexamethasone Degradation in Aqueous Medium and Implications for Correction of In Vitro Release from Sustained Release Delivery Systems. *AAPS PharmSciTech* **2019**, *20*, 320.

(42) Dunn, K. C.; Aotaki-Keen, A. E.; Putkey, F. R.; Hjelmeland, L. M. ARPE-19, a human retinal pigment epithelial cell line with differentiated properties. *Exp. Eye Res.* **1996**, *62*, 155–170.

(43) Masuda, N.; Tsujinaka, H.; Hirai, H.; Yamashita, M.; Ueda, T.; Ogata, N. Effects of concentration of amyloid  $\beta$  ( $A\beta$ ) on viability of cultured retinal pigment epithelial cells. *BMC Ophthalmol.* **2019**, *19*, 70.

## Recommended by ACS

### Chitosan Hydrogels with Embedded Thermo- and pH-Responsive Microgels as a Potential Carrier for Controlled Release of Drugs

Nirbhai Singh, Abhijit Dan, et al.

JUNE 21, 2022  
ACS APPLIED BIO MATERIALS

READ 

### Hyaluronic Acid-PEG-Based Diels–Alder *In Situ* Forming Hydrogels for Sustained Intraocular Delivery of Bevacizumab

Blessing C. Ilochonwu, Tina Vermonden, et al.

JUNE 23, 2022  
BIOMACROMOLECULES

READ 

### Photodynamic Lignin Hydrogels: A Versatile Self-Healing Platform for Sustained Release of Photosensitizer Nanoconjugates

Sanjam Chandna, Jayeeta Bhaumik, et al.

NOVEMBER 14, 2022  
ACS APPLIED POLYMER MATERIALS

READ 

### Degradable Bioadhesives Based on Star PEG–PLA Hydrogels for Soft Tissue Applications

Mathilde Grosjean, Benjamin Nottelet, et al.

DECEMBER 16, 2022  
BIOMACROMOLECULES

READ 

Get More Suggestions >